Dynamic analysis of a coinfection model of dengue and asymptomatic and symptomatic COVID-19

Atikah Lamis[1] and *Hengki* Tasman[1,*]

[1]Department of Mathematics, Faculty of Mathematics and Natural Sciences (FMIPA), Universitas Indonesia, Kampus UI Depok, Depok 16424, Indonesia.

Abstract. The purpose of this paper is to investigate the transmission dynamics of COVID-19 with Dengue coinfection using a mathematical model. The human population was divided into six compartments, while the mosquito population was divided into two sections. The model considers that COVID-19 infection might be symptomatic or asymptomatic. First, we analyzed the dengue infection model. The basic reproduction number of the COVID-19 infection system and the Dengue infection system are used to forecast illness mitigation and persistence (denoted by $\mathcal{R}_{0C}$ and $\mathcal{R}_{0D}$ respectively). The qualitative examination of the sub-systems indicated that the disease-free equilibrium (DFE) is locally asymptotically stable provided the corresponding reproduction numbers are less than one. The coinfection model is then analyzed to yield the basic reproduction number, designated by $\mathcal{R}_0$. The DFE and stability of the coinfection model are dependent on $\mathcal{R}_0 = \max\{\mathcal{R}_{0D}, \mathcal{R}_{0C}\}$. The numerical simulation of the coinfection model showed the existence of the endemic equilibrium of the coinfection model. Furthermore, we studied the dynamic solutions of the coinfection model by establishing the equilibrium points and evaluated the stability requirements.

Keywords. COVID-19, dengue, mathematical model, coinfection, basic reproduction number

1 Introduction

On December 31, 2019, the World Health Organization (WHO) initially reported a coronavirus (COVID-19) epidemic as pneumonia of unknown cause in Wuhan, China [1]. COVID-19 is a respiratory virus that spreads by contact with saliva droplets expelled by an infected person while coughing or sneezing [2]. While Dengue is transmitted to humans by *Aedes sp.* mosquitoes [3]. COVID-19 and Dengue may share clinical and laboratory features [4]. The first confirmed case of dengue fever with COVID-19 coinfection was reported in a French overseas department in the Indian Ocean [5], and a female aged 62 years in the Philippines who presented at the emergency department with suspected COVID-19 and suspicion of dengue fever [6].

Four dengue virus serotypes cause dengue fever, these are, DENV-1, DENV-2, DENV-3, and DENV-4. The virus is a member of the Flaviviridae family [7]. The virus is transmitted by

*Corresponding author: htasman@sci.ui.ac.id

infected *Aedes sp.* mosquito to humans. When a person is infected with dengue, It can induce dengue fever, a nonspecific febrile sickness. Because of urbanization, international travel, and other factors, dengue infection has rapidly spread to all parts of the world (mainly tropical and subtropical countries), and it currently threatens one-third of the world's population every year [8].

Infections with COVID-19 might be symptomatic or asymptomatic [9]. One of the factors leading to the difficulty in controlling the COVID-19 pandemic is the infectious status of persons who are asymptomatic or have only minor symptoms [9]. Asymptomatic COVID-19 infections were shown to have a similar viral burden as symptomatic infections [10]. Close contact with proven cases increases the possibility of contracting a viral infection without showing clinical symptoms. Some people infected with coronavirus may have no symptoms or only mild symptoms during the disease's incubation period and may go undetected.

These hidden coronavirus cases may be unaware of their infection, but when tested using reverse transcriptase polymerase chain reaction (RT-PCR) [11], they are verified as positive cases. If there were a large proportion of asymptomatic carriers and the coronavirus was as contagious as symptomatic patients, it would constitute a significant threat to global public health.

Infectious disease behavior has been studied using mathematical models. Moreover, various research has offered mathematical assessments of symptomatic and asymptomatic COVID-19 infection. Arcede *et al* in [12] proposed an extension from the traditional SEIR model by including an asymptomatic infected compartment. Ahmed in [13] created a simple mathematical model with asymptomatic and symptomatic classifications to examine transmission and control. Biswas in [14] modeled the effect of self-immunity and the impacts of asymptomatic and symptomatic individuals on COVID-19.

Many models have examined coinfection between COVID-19 or Dengue and other infectious diseases. The simultaneous infection of an individual as a result of the appearance of more than one infectious disease in the same location is known as coinfection, for instance, TB and COVID-19 [15], COVID-19 and cholera [16], dengue and leptospirosis [17], COVID-19 and diabetes [18], COVID-19 and HIV infection [19], dengue and Zika [20].

Several investigations on COVID-19 and dengue coinfection models have recently been conducted. The first such paper cited here is Omame *et al* [21], in which they build and analyze an acceptable mathematical model for the dynamics of COVID-19 and dengue transmission in Brazil, including optimal control and cost-effectiveness evaluations. In the same way, optimal control and data-driven analysis [5] creates and tests a highly effective mathematical model for COVID-19 co-infection and dengue transmission dynamics. The impact of coinfection, particularly in dengue or COVID-19 endemic areas, might lead to the outbreak of an epidemic, thereby overburdening a country's healthcare infrastructure. In response to the preceding issues, we created a mathematical model that determines Dengue and COVID-19 coinfection containing asymptomatic and symptomatic classes to study their dynamics.

This article is presented as follows. This section briefly reviews the literature and the current state of our research. Section 2 contains directions for constructing the mathematical model. In Section 3, model analysis of the COVID-19 infection only, dengue infection only, and the coinfection. The basic reproduction numbers of the three systems are also determined. The existence and local stability of the dengue-endemic equilibrium point are then investigated in section 4. In the final section, we share a few key findings from our research.

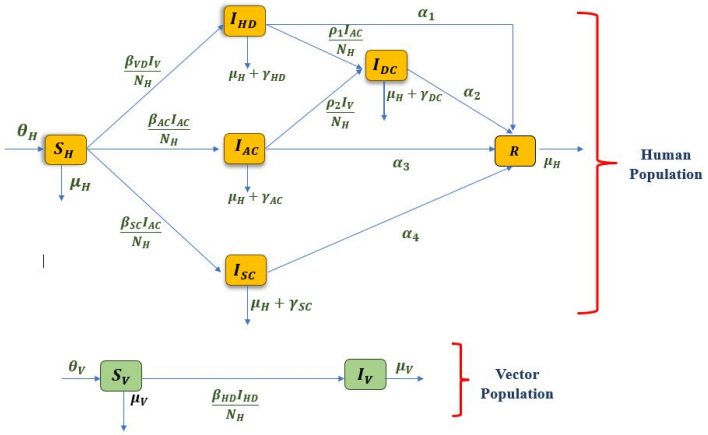

Fig. 1. Transmission diagram of COVID-19-dengue coinfection.

2 Mathematical model formulation

A model for the coinfection of Dengue-COVID-19 was formulated by subdividing the population. For our model, we divide the human population into six subpopulations and the mosquito population into two subpopulations.. The subpopulations are shown in Table 1.

We expected that the recruitment rate θ_H increases the susceptible human. Because we assumed all symptomatic COVID-19-infected humans were isolated, the susceptible human can become dengue-infected through contact with dengue-only infected vectors and acquire COVID-19 infection through contact with only asymptomatic COVID-19 infected humans, COVID-19 infected maybe I_{AC} or I_{SC}. The dengue-infected human population $_{HD}$ recovers at a rate of α_1, transfers to the coinfection-class at a force of infection of ρ_1, or dies from dengue-induced death at a rate of γ_{HD}. We also assume that dengue-infected persons only become coinfected after coming into touch with I_{AC}. The population of asymptomatic COVID-19 infected $_{AC}$ recovers at an α_3 rate and moves to the coinfection class at a ρ_2 rate, or dies from COVID-19 at a rate γ_{AC}. Humans in I_{SC} and I_{DC} classes recovers at rate α_4 and α_2 respectively respectively. This model does not account for the risk of reinfection following recovery. Natural death is expected to decrease all human compartments at a constant rate of mu_H.

Table. 1. Description of subpopulations or variables.

Variable	Description	Unit
S_H	Susceptible human subpopulation	Human
I_{HD}	Dengue-infected human subpopulation	Human
I_{AC}	Asymptomatic COVID-19-infected subpopulation	Human
I_{SC}	Symptomatic COVID-19-infected subpopulation	Human
I_{DC}	Dengue-COVID-19-infected subpopulation	Human
R	Recovered human subpopulation	Human
S_V	Susceptible mosquito subpopulation	Mosquito
I_V	Dengue-infected mosquito subpopulation	Mosquito

As already mentioned, the entire mosquito population is divided only into susceptible and infected mosquitoes. The number of susceptible mosquitoes increases at a constant rate of θ_V and decreases during dengue infection. Susceptible mosquitoes transmit dengue fever at a constant rate of β_{HD} in I_{HD} after biting an infected person. Furthermore, the natural death rate μ_V reduces the quantity of susceptible and infected mosquitoes.

We construct the following system of nonlinear ordinary differential equations describing the dynamics of dengue and COVID-19 co-infection from Fig. 1.

$$\begin{aligned}
\frac{dS_H}{dt} &= \theta_H - \Big(\frac{\beta_{VD}I_V}{N_H} + \frac{\beta_{AC}I_{AC}}{N_H} + \frac{\beta_{SC}I_{AC}}{N_H}\Big)S_H - \mu_H S_H,\\
\frac{dI_{HD}}{dt} &= \frac{\beta_{VD}I_V}{N_H}S_H - \frac{\rho_1 I_{AC}}{N_H}I_{HD} - \alpha_1 I_{HD} - (\mu_H + \gamma_{HD})I_{HD},\\
\frac{dI_{SC}}{dt} &= \frac{\beta_{SC}I_{AC}}{N_H}S_H - \alpha_4 I_{SC} - (\mu_H + \gamma_{SC})I_{SC},\\
\frac{dI_{AC}}{dt} &= \frac{\beta_{AC}I_{AC}}{N_H}S_H - \frac{\rho_2 I_V}{N_H}I_{AC} - \alpha_3 I_{AC} - (\mu_H + \gamma_{AC})I_{AC},\\
\frac{dI_{DC}}{dt} &= \frac{\rho_1 I_{AC}}{N_H}I_{HD} + \frac{\rho_2 I_V}{N_H}I_{AC} - \alpha_2 I_{DC} - (\mu_H + \gamma_{DC})I_{DC}\\
\frac{dR}{dt} &= \alpha_1 I_{HD} + \alpha_2 I_{DC} + \alpha_3 I_{AC} + \alpha_4 I_{SC} - \mu_H R,\\
\frac{dS_V}{dt} &= \theta_v - \frac{\beta_{HD}I_{HD}}{N_H}S_V - \mu_v S_V,\\
\frac{dI_V}{dt} &= \frac{\beta_{HD}I_{HD}}{N_H}S_V - \mu_V I_V,
\end{aligned} \tag{1}$$

where $N_H = S_H + I_{HD} + I_{SC} + I_{AC} + I_{DC} + R$ is the total population of humans. A description of the system's parameters is shown in Table 2. All of the parameters are positive and constant.

3 Analysis of system

To understand the dynamics of System (1), we determined the system's equilibrium points and analyze their stability. The analysis will be carried out in three parts, by looking into the behaviour of the COVID-19 infection system, the Dengue infection system and the Dengue-COVID-19 coinfection system.

3.1 COVID-19 infection system

Without considering the dengue infection, System (1) could be reduced into the following system.

$$\begin{aligned}
\frac{dS_H}{dt} &= \theta_H - \Big(\frac{\beta_{AC}I_{AC}}{N_H} + \frac{\beta_{SC}I_{AC}}{N_H}\Big)S_H - \mu_H S_H,\\
\frac{dI_{SC}}{dt} &= \frac{\beta_{SC}I_{AC}}{N_H}S_H - \alpha_4 I_{SC} - (\mu_H + \gamma_{SC})I_{SC},\\
\frac{dI_{AC}}{dt} &= \frac{\beta_{AC}I_{AC}}{N_H}S_H - \alpha_3 I_{AC} - (\mu_H + \gamma_{AC})I_{AC},\\
\frac{dR}{dt} &= \alpha_3 I_{AC} + \alpha_4 I_{SC} - \mu_H R,
\end{aligned} \tag{2}$$

Table. 2. Description of the parameters.

Parameter	Description	Unit
θ_H	Recruitment rate of human	$\frac{human}{day}$
β_{VD}	Effective contact rate for vector to human transmission of dengue	$\frac{1}{day}$
β_{AC}	Effective contact rate for human to human transmission of asymptomatic COVID-19 infection	$\frac{1}{day}$
β_{SC}	Effective contact rate for human to human transmission of symptomatic COVID-19 infection	$\frac{1}{day}$
ρ_1	Effective contact rate of dengue individuals to the coinfected class	$\frac{1}{day}$
ρ_2	Effective contact rate of asymptomatic COVID-19 individuals to the coinfected class	$\frac{1}{day}$
α_1	Recovery rate of dengue infection	$\frac{1}{day}$
α_2	Recovery rate of coinfection	$\frac{1}{day}$
α_3	Recovery rate of asymptomatic COVID-19 infection	$\frac{1}{day}$
α_4	Recovery rate of symptomatic COVID-19 infection	$\frac{1}{day}$
μ_H	Natural death rate of human	$\frac{1}{day}$
γ_{DC}	Human death rate of coinfection	$\frac{1}{day}$
γ_{HD}	Human death rate of dengue infection	$\frac{1}{day}$
γ_{AC}	Death rate of asymptomatic COVID-19 infection	$\frac{1}{day}$
γ_{SC}	Death rate of symptomatic COVID-19 infection	$\frac{1}{day}$
β_{HD}	Effective contact rate for human to vector transmission of Dengue	$\frac{1}{day}$
μ_V	Natural death rate of mosquito	$\frac{1}{day}$
θ_V	Recruitment rate of mosquito	$\frac{mosquito}{day}$

where $N_H = S_H + I_{SC} + I_{AC} + R$. The biological domain of system (2) is,

$$\Omega_C = \left\{ (S_H, I_{SC}, I_{AC}, R) \in \mathbb{R}^4_+ : 0 < N_H \leq \frac{\theta_H}{\mu_H} \right\}. \tag{3}$$

System (2) has the disease-free equilibrium (DFE),

$$\epsilon_{0C} = \left(S^0_H, I^0_{SC}, I^0_{AC}, R^0 \right) = \left(\frac{\theta_H}{\mu_H}, 0, 0, 0 \right).$$

The average number of secondary infections induced by a single COVID-19 infected individual in a susceptible population is defined as the basic reproduction number of System (2). Using the next-generation matrix method [22], we determined the basic reproduction number of System (2).

Theorem 1. *The basic reproduction number of the COVID-19 infection system (2) is,*

$$\mathcal{R}_{0C} = \frac{\beta_{AC}}{\alpha_3 + \gamma_{AC} + \mu_H}. \tag{4}$$

The local stability of the disease-free equilibrium points of COVID-19 ϵ_{0C} is as follows.

Theorem 2. *The disease-free equilibrium point ϵ_{0C} is locally asymptotically stable if $\mathcal{R}_{0C} <$ 1, and it is unstable if $\mathcal{R}_{0C} > 1$.*

Proof. The Jacobian matrix of system (2) at ϵ_{0C} is given by,

$$J(\epsilon_{0C}) = \begin{bmatrix} -\mu_H & 0 & -\beta_{AC} - \beta_{SC} & 0 \\ 0 & -\alpha_4 - \gamma_{SC} - \mu_H & \beta_{SC} & 0 \\ 0 & 0 & -\alpha_3 + \beta_{AC} - \mu_H & 0 \\ 0 & \alpha_4 & \alpha_3 & -\mu_H \end{bmatrix}. \tag{5}$$

The Jacobian matrix $J(\epsilon_{0C})$ has eigenvalues $\lambda_{1,2} = -\mu_H$, $\lambda_3 = -(\alpha_4 + \gamma_{SC} + \mu_H)$, and $\lambda_4 = -\alpha_3 + \beta_{AC} - \gamma_{AC} - \mu_H = (\mathcal{R}_{0C} - 1)(\alpha_3 + \gamma_{AC} + \mu_H)$.

We needed λ_4 which is equivalent to $\mathcal{R}_{0C}$, for local asymptotic stability. Thus, if $\mathcal{R}_{0C}$, the disease-free equilibrium ϵ_{0C} is locally asymptotically stable. □

System (2) has an endemic equilibrium point $\epsilon_C = \left(S_H^*, I_{HD}^*, R^*, S_V^*, I_V^*\right)$, where

$$\begin{aligned} S_H^* &= \frac{\theta_H(\beta_{SC}(\alpha_4 + \mu_H) + \mathcal{R}_{0C}(\alpha_3 + \mu_H)(\alpha_4 + \mu_{SC} + \mu_H))}{\mu_H(\Phi)}, \\ I_{SC}^* &= \frac{(\mathcal{R}_{0C} - 1)\beta_{SC}\theta_H}{\Phi}, \\ I_{AC}^* &= \frac{(\mathcal{R}_{0C} - 1)\mathcal{R}_{0C}\theta_h(\alpha_4 + \gamma_{SC} + \mu_h)}{\Phi}, \\ R^* &= \frac{(\mathcal{R}_{0C} - 1)\theta_H(\alpha_4\beta_{SC} + \mathcal{R}_{0C}\alpha_3(\alpha_4 + \gamma_{SC} + \mu_H))}{\mu_H\Phi}, \end{aligned}$$

and $\Phi = \alpha_4(\beta_{SC} + \mu_H) + \mu_H(\beta_{SC} + \gamma_{SC} + \mu_H) + (\mathcal{R}_{0C} - 1)(\beta_{AC}(\alpha_4 + \gamma_{SC} + \mu_H) + \beta_{SC}\gamma_{SC})$. It is clear that the endemic equilibrium point exists if $\mathcal{R}_{0C} > 1$.

Theorem 3. *The system (2) has an endemic equilibrium ϵ_C if $\mathcal{R}_{0C} > 1$.*

3.2 Dengue infection system

Excluding the COVID-19 infection from the Dengue-COVID-19 coinfection system (1), we obtain Dengue infection system as follows.

$$\begin{aligned} \frac{S_H}{dt} &= \theta_H - \left(\frac{\beta_{VD} I_V}{N_H}\right) S_H - \mu_H S_H, \\ \frac{I_{HD}}{dt} &= \frac{\beta_{VD} I_V}{N_H} S_H - \alpha_1 I_{HD} - (\mu_H + \gamma_{HD}) I_{HD}, \\ \frac{dR}{dt} &= \alpha_1 I_{HD} - \mu_H R, \\ \frac{dS_V}{dt} &= \theta_v - \frac{\beta_{HD} I_{HD}}{N_H} S_V - \mu_V S_V, \\ \frac{dI_V}{dt} &= \frac{\beta_{HD} I_{HD}}{N_H} S_V - \mu_V I_V, \end{aligned} \tag{6}$$

where $N_H = S_H + I_{hd} + R$ and $N_V = S_V + I_V$. The biological region for system (6) is,

$$\Omega_D = \left\{ (S_H, I_{HD}, I_R, R.S_V, I_V) \in \mathbb{R}_+^5 : N_H \leq \frac{\theta_H}{\mu_H}; N_V(t) \leq \frac{\theta_V}{\mu_V} \right\}.$$

System (6) has a disease-free equilibrium (DFE),

$$\epsilon_{D0} = \left(S_H^0, I_{HD}^0, R^0, S_V^0, I_V^0\right) = \left(\frac{\theta_H}{\mu_H}, 0, 0, \frac{\theta_V}{\mu_V}, 0\right) \tag{7}$$

We calculated the basic reproduction number $\mathcal{R}_{0D}$ of the Dengue system (6) using the next generation matrix method [22]. As a result, we get the following result.

Theorem 4. *The basic reproduction number of the Dengue infection system (6) is,*

$$\mathcal{R}_{0D} = \frac{1}{\mu_V}\sqrt{\frac{\beta_{HD}\mu_H\theta_V\beta_{VD}}{\theta_H(\alpha_1+\mu_H+\gamma_{HD})}}. \tag{8}$$

To examine the local stability analysis of the disease-free equilibrium ϵ_{D0}, we used the linearization approach. First, we determined the Jacobian matrix of Dengue infection system (6) at ϵ_{D0}. Three eigenvalues of the matrix are $\lambda_{1,2,3} = -\mu_H$, and the other two eigenvalues are obtained from the submatrix of the Jacobian matrix,

$$J_2 = \begin{bmatrix} -\alpha_1-\gamma_{HD}-\mu_H & \beta_{VD} \\ \frac{\beta_{HD}\theta_V\mu_H}{\theta_H\mu_V} & -\mu_V \end{bmatrix}.$$

If the trace of the submatrix is negative and its determinant is positive, the other two eigenvalues are negative [23]. The trace is $tr(J_2) = -(\alpha_1+\gamma_{HD}-\mu_H-\mu_V) < 0$. The determinant is $\det(J_1) = -\frac{\beta_{HD}\beta_{VD}\theta_V\mu_H}{\theta_H\mu_V}+\alpha_1\mu_V+\gamma_{HD}\mu_V+\mu_H\mu_V = -((\mathcal{R}_{0D}-1)(\alpha_1+\gamma_{HD}+\mu_H)\mu_V)$. The sign of the determinant is positive if $\mathcal{R}_{0D} < 1$ and $\det(J_2) < 0$ if $\mathcal{R}_{0D} > 1$. The following theorem follows.

Theorem 5. *The disease-free equilibrium ϵ_{D0} of the dengue infection System* (6) *is locally asymptotically stable if $\mathcal{R}_{0D} < 1$, and it is unstable if $\mathcal{R}_{0D} > 1$.*

The parameter values in Table 3 are used for conducting a numerical experiment on the existence and stability of the dengue-infected system's endemic equilibrium (6). Using this set of parameters, we obtain $\mathcal{R}_{0D} = 2.138$, which is larger than one. As a result, according to Theorem 5, the disease-free equilibrium ϵ_{0D} is unstable. Substituting all of the system parameters (6) results in:

$$\begin{aligned}
\frac{dS_H}{dt} &= 2110016 - 0.0078S_H - 0.43\frac{I_V S_H}{N_H}, \\
\frac{dI_{HD}}{dt} &= 0.43\frac{I_v S_H}{N_H} - 0.83I_{HD}, \\
\frac{dR}{dt} &= 0.15I_{HD} - 0.0078R, \\
\frac{dS_V}{dt} &= 20000 - \frac{0.6I_{HD}}{N_H}S_V - 0.071S_V, \\
\frac{dI_V}{dt} &= \frac{0.6I_{HD}}{N_H}S_V - 0.071I_V.
\end{aligned} \tag{9}$$

We set the system's right side (9) to zero and solve it with all variables. This produces a disease-free equilibrium as follows:

$$\epsilon_{D1} = (S_H, I_{HD}, R, S_V, I_V) = \left(2.70515\times10^7, 0, 0, 2.8169\times10^6, 0\right),$$

The endemic equilibrium is represented by:

$$\epsilon_{D2} = (S_H, I_{HD}, R, S_V, I_V) = \left(1.63\times10^7, 1.011\times10^6, 1.94\times10^6, 518754, 2.3\times10^6\right).$$

We linearized System (9) on the equilibrium point to examine the local stability of each equilibrium. The Jacobian matrix of System (9) at ϵ_{D1} yields,

$$J(\epsilon_{D1}) = \begin{bmatrix} -0.078 & 0 & 0 & 0 & 0.43 & \\ 0 & -0.828 & 0 & 0 & 0.43 & \\ 0 & 0.15 & -0.078 & 0 & 0 & \\ 0 & -0.062 & 0 & -0.0071 & 0 & \\ 0 & 0.0625 & 0 & 0 & 0 & -0.0071 \end{bmatrix}. \tag{10}$$

The eigenvalues of $J(\epsilon_{D1})$ are,

$$\lambda_1 = -0.86, \lambda_{2,3} = -0.078, \lambda_4 = 0.0244172, \lambda_5 = -0.0071,$$

Since $\lambda_4 > 0$, we determine that ϵ_{D1} is unstable.

Using the same technique, Matrix (11) obtains the Jacobian matrix of the System (9) on ϵ_2.

$$J(\epsilon_{D2}) = \begin{bmatrix} -0.086 & 0.043 & 0.043 & 0 & -0.364 \\ 0.0076 & -0.87 & -0.043 & 0 & 0.364 \\ 0 & 0.15 & 0.078 & 0 & 0 \\ 8.46 * 10^4 & -0.015 & 8.46 * 10^4 & -0.038 & 0 \\ -8.46 * 10^4 & 0.015 & -8.46 * 10^4 & 0.03124 & -0.0071 \end{bmatrix}. \tag{11}$$

with eigenvalues,

$$\lambda_1 = -0.87, \lambda_2 = -0.096, \lambda_3 = -0.078, \lambda_4 = -0.03, \lambda_5 = 0.0071$$

We can determine that ϵ_{D2} is locally asymptotically stable given a set of parameters such that $\mathcal{R}_{0C} > 1$ since all of the eigenvalues are negative.

3.3 Dengue–COVID-19 coinfection model

System (1) is the dengue and COVID-19 coinfection model. For this model the total human population is $N_H = S_H + I_{HD} + I_{SC} + I_{AC} + I_{DC} + R$ and the total mosquito population is $N_V = S_V + I_V$. The disease-free equilibrium point of the whole model (ϵ_0) is then calculated as follows:

$$\epsilon_0 = (S_H^0, I_{HD}^0, I_{SC}^0, I_{AC}^0, I_{DC}^0, R^0, S_V^0, I_V^0) = \Big(\frac{\theta_H}{\mu_H}, 0, 0, 0, 0, 0, \frac{\theta_V}{\mu_V}, 0\Big) \tag{12}$$

We have now estimated the basic reproduction number $\mathcal{R}_0$ of the complete model using the next generation matrix approach [22] as follows. To express the vector function, we use the notation $x = (I_{HD}, I_{SC}, I_{SC}, I_{AC}, I_{DC}, I_V, R)$:

$$\mathcal{F} = \begin{bmatrix} \frac{\beta_{VD} I_V}{N_H} S_H \\ \frac{\beta_{SC} I_{AC}}{N_H} S_H \\ \frac{\beta_{AC} I_{AC}}{N_H} S_H \\ 0 \\ \frac{\beta_{HD} I_{HD}}{N_H} S_H \\ 0 \end{bmatrix} \text{ and } \mathcal{V} = \begin{bmatrix} -\frac{\rho_1 I_{AC}}{N_H} I_{HD} - \alpha_1 I_{HD} - (\mu_H + \gamma_{HD}) I_{HD} \\ -\alpha_4 I_{SC} - (\mu_H + \gamma_{SC}) I_{SC} \\ -\frac{\rho_2 I_V}{N_H} I_{AC} - \alpha_3 I_{AC} - (\mu_H + \gamma_{AC}) I_{AC} \\ \frac{\rho_1 I_{AC}}{N_H} I_{HD} + \frac{\rho_2 I_V}{N_H} I_{AC} - \alpha_2 I_{DC} - (\mu_H + \gamma_{DC}) I_{DC} \\ -\mu_V I_V \\ \alpha_1 I_{HD} + \alpha_2 I_{DC} + \alpha_3 I_{AC} + \alpha_4 I_{SC} - \mu_H R \end{bmatrix},$$

depicting the emergence of new infections and the movement of individuals into and out of infected compartments.

The corresponding Jacobian matrix of $\mathcal{F}$ evaluated at the dengue-free equilibrium ϵ_0 is given by:

$$F(\epsilon_0) = \begin{bmatrix} -\alpha_1 - \gamma_{HD} - \mu_H & 0 & 0 & 0 & 0 & 0 \\ 0 & -\alpha_4 - \gamma_{SC} - \mu_H & 0 & 0 & 0 & 0 \\ 0 & 0 & -\alpha_3 - \gamma_{AC} - \mu_H & 0 & 0 & 0 \\ 0 & 0 & 0 & -\alpha_2 - \gamma_{DC} - \mu_H & 0 & 0 \\ 0 & 0 & 0 & 0 & -\mu_V & 0 \\ 0 & \alpha_4 & \alpha_3 & 0 & 0 & -\mu_H \end{bmatrix}.$$

and the Jacobian matrix of $\mathcal{V}$ assessed at the dengue-free equilibrium ϵ_0 is given by:

$$V = \begin{bmatrix} -\frac{1}{\alpha_1+\gamma_{HD}+\mu_H} & 0 & 0 & 0 & 0 & 0 \\ 0 & -\frac{1}{\alpha_4+\gamma_{SC}+\mu_H} & 0 & 0 & 0 & 0 \\ 0 & 0 - \frac{1}{\alpha_3+\gamma_{AC}+\mu_H} & 0 & 0 & 0 & \\ 0 & 0 & 0 & -\frac{1}{\alpha_2+\gamma_{DC}+\mu_H} & 0 & 0 \\ 0 & 0 & 0 & 0 & -\frac{1}{\mu_V} & 0 \\ 0 & -\frac{\alpha_4}{\mu_H(\alpha_4+\gamma_{SC}+\mu_H)} & -\frac{\alpha_3}{\mu_H(\alpha_3+\gamma_{AC}+\mu_H)} & 0 & 0 & -\frac{1}{\mu_H} \end{bmatrix}.$$

The basic reproduction number from the product matrix $K = -FV - 1$ is then the greatest of the eigenvalues shown below.

$$\lambda_{1,2,3} = 0, \lambda_4 = \frac{\beta_{AC}}{\alpha_3 + \gamma_{AC} + \mu_H},$$

$$\Lambda_5 = -\frac{1}{\mu_V} \cdot \sqrt{\frac{\beta_{HD}\mu_H\theta_V\beta_{VD}}{\theta_H(\alpha_1 + \mu_H + \gamma_{HD})}}, \Lambda_6 = \frac{1}{\mu_V} \cdot \sqrt{\frac{\beta_{HD}\mu_H\theta_V\beta_{VD}}{\theta_H(\alpha_1 + \mu_H + \gamma_{HD})}}.$$

As a result, the basic reproductive number of the coinfection system is,

$$\mathcal{R}_{0CD} = \max\{\mathcal{R}_{0C}, \mathcal{R}_{0D}\}. \tag{13}$$

Using the linearization method, we performed a local stability study of the disease-free equilibrium point of the complete model. At ϵ_0, the Jacobian matrix of the entire System (1) is given by,

$$J(\epsilon_0) = \begin{bmatrix} -\mu_H & 0 & 0 & -\beta_{AC} - \beta_{SC} & 0 & 0 & 0 & -\beta_{VD} \\ 0 & \vartheta_1 & 0 & 0 & 0 & 0 & 0 & \beta_{VD} \\ 0 & 0 & -\alpha_4 - \gamma_{SC} - \mu_H & \beta_{SC} & 0 & 0 & 0 & 0 \\ 0 & 0 & 0 & \vartheta_2 & 0 & 0 & 0 & 0 \\ 0 & 0 & 0 & 0 & \alpha_2 - \gamma_{DC} - \mu_H & 0 & 0 & 0 \\ 0 & \alpha_1 & \alpha_4 & \alpha_3 & \alpha_2 & -\mu_H & 0 & 0 \\ 0 & -\frac{\beta_{HD}\theta_V\mu_H}{\theta_H\mu_V} & 0 & 0 & 0 & 0 & -\mu_v & 0 \\ 0 & \frac{\beta_{HD}\theta_V\mu_H}{\theta_H\mu_V} & 0 & 0 & 0 & 0 & 0 & -\mu_V \end{bmatrix}. \tag{14}$$

Where $\vartheta_1 = -\alpha_1 - \gamma_{HD} - \mu_H$ and $\vartheta_2 = -\alpha_3 + \beta_{AC} - \gamma_{AC} - \mu_H$. From Equation (14), we get the following characteristic polynomial.

$$\begin{aligned} p(\lambda) \quad = \quad & [\lambda + \mu_H]^2 [\lambda + \mu_V] [\lambda + (\alpha_2 + \gamma_{DC} + \mu_H)] [\lambda + \alpha_4 + \gamma_{SC} + \mu_H] \\ & [\lambda + (1 - \mathcal{R}_{0C})(\alpha_3 + \gamma_{AC} + \mu_H)] [\lambda^2 + (1 - \mathcal{R}_{0D}) \\ & (\alpha_1 + \gamma_{HD} + \mu_H)\mu_V\lambda + (\alpha_1 + \gamma_{HD} + \mu_H + \mu_V)]. \end{aligned}$$

Table. 3. The parameter values of Model (1) for numerical simulation.

Parameter	Value	Source	Parameter	Value	Source
θ_H	2110016	[24]	α_3	0.12	[12]
β_{VD}	0.43	[25]	α_4	0.1853	[26]
β_{AC}	0.8	Assumed	μ_H	0.0078	[14]
β_{SC}	0.2	Assumed	γ_{DC}	0.2	Assumed
ϕ_1	0.3	Assumed	γ_{HD}	0.6	Assumed
ϕ_2	0.3	Assumed	γ_{AC}	0.2	Assumed
α_1	0.15	[27]	γ_{SC}	0.023	[28]
α_2	0.5	Assumed	β_{HD}	0.6	[25]
μ_V	0.071	[17]	θ_V	20000	[26]

The eigenvalues are,

$$\lambda_{1,2} = -\mu_H,\ \lambda_3 = -\mu_V,\ \lambda_4 = -(\alpha_2 + \gamma_{DC} + \mu_H),$$
$$\lambda_5 = (\mathcal{R}_{0C} - 1)(\alpha_3 + \gamma_{AC} + \mu_H),\ \lambda_6 = -(\alpha_2 + \gamma_{DC} + \mu_H).$$

It is clear that λ_5 is negative if $\mathcal{R}_{0C} > 1$. Let λ_7 and λ_8 be other two eigenvalues, $\lambda_7, \lambda_8 < 0$ if $\lambda_7 \cdot \lambda_8 > 0$ and $\lambda_7 + \lambda_8 < 0$. Hence, all eigenvalues are negative if $\mathcal{R}_{0C} > 1$ and $\mathcal{R}_{0D} > 1$. Therefore, Dengue-COVID-19 is locally asymptotically stable if $\mathcal{R}_{0CD} = \max\{\mathcal{R}_{0C}, \mathcal{R}_{0D}\} < 1$. Then, we obtain the following theorem.

Theorem 6. *The disease-free equilibrium point of the Dengue-COVID-19 Coinfection Model (1) is locally asymptotically stable if $\mathcal{R}_{0CD} < 1$, and it is unstable if $\mathcal{R}_{0CD} > 1$.*

The same parameter settings are utilized in Table 3 for conducting a numerical experiment on the existence and stability of the coinfection model's endemic equilibrium in the System (1).

Using this set of parameters, we got $\mathcal{R}_0 = \max\{\mathcal{R}_{0C} = 1.67, \mathcal{R}_{0D} = 2.138\}$, which is larger than one. As a result, according to Theorem 6, the disease-free equilibrium ϵ_0 is unstable. Substituting all of the parameters on the System (1) yields:

$$\begin{aligned}
\frac{dS_H}{dt} &= 2110016 - \Big(\frac{0.43I_V}{N_H} + \frac{0.8I_{AC}}{N_H} + \frac{0.2I_{AC}}{N_H}\Big)S_H - 0.0078S_H,\\
\frac{dI_{HD}}{dt} &= 0.43I_V S_H N_H S_H - \frac{0.3I_{AC}}{N_H} I_{HD} - 0.15I_{HD} - (0.0078 + 0.6)I_{HD},\\
\frac{dI_{SC}}{dt} &= \frac{0.2I_{AC}}{N_H} S_H - 0.1853I_{SC} - 0.0308I_{SC},\\
\frac{dI_{AC}}{dt} &= \frac{0.8I_{AC}}{N_H} S_H - \frac{0.3I_V}{N_H} I_{AC} - 0.12I_{AC} - 0.2078I_{AC},\\
\frac{dI_{DC}}{dt} &= \frac{0.3}{N_H} I_{HD} + \frac{0.3I_V}{N_H} I_{AC} - 0.5I_{DC} - 0.2078I_{DC}\\
\frac{dR}{dt} &= 0.15I_{HD} + 0.5I_{DC} + 0.12I_{AC} + 0.1853I_{SC} - 0.0078R,\\
\frac{dS_V}{dt} &= 20000 - \frac{0.6I_{HD}}{N_H} S_V - 0.071S_V,\\
\frac{dI_V}{dt} &= \frac{0.6I_{HD}}{N_H} S_V - 0.071I_V.
\end{aligned} \tag{15}$$

We solve the problem by setting the right-hand side (15) to zero. As a result, there is a disease-free homeostasis.

$$\epsilon_1 = (S_H, I_{HD}, I_{SC}, I_{AC}, I_{DC}, R, S_V, I_V) = \Big(2.70515 \times 10^7, 0, 0, 0, 0, 0, 2.8169 \times 10^6, 0\Big),$$

and the endemic equilibrium,

$$\begin{aligned} \epsilon_2 &= (S_H, I_{HD}, I_{SC}, I_{AC}, I_{DC}, R, S_V, I_V) \\ &= \Big(1.2 \times 10^8, 6.5 \times 10^3, 4.5 \times 10^5, 1.1 \times 10^8, 2.9 \times 10^4, 5.2 \times 10^9, \\ &\quad 7.3 \times 10^6, 2.1 \times 10^6\Big). \end{aligned}$$

To investigate the local stability of each equilibrium, we linearize the System (15) on the equilibrium point. The System's Jacobian matrix (15) at ϵ_1 gives,

$$J(\epsilon_1) = \begin{bmatrix} -0.078 & 0 & 0 & -1 & 0 & 0 & 0 & -0.43 \\ 0 & -0.828 & 0 & 0 & 0 & 0 & 0 & 0.43 \\ 0 & 0 & -0.286 & 0.2 & 0 & 0 & 0 & 0 \\ 0 & 0 & 0 & 0.322 & 0 & 0 & 0 & 0 \\ 0 & 0 & 0 & 0 & -0.778 & 0 & 0 & 0 \\ 0 & 0.15 & 0.185 & 0.2 & 0.5 & -0.078 & 0 & 0 \\ 0 & -0.062 & 0 & 0 & 0 & 0 & -0.0071 & 0 \\ 0 & 0.0625 & 0 & 0 & 0 & 0 & 0 & -0.0071 \end{bmatrix}. \tag{16}$$

The eigenvalues of $J(\epsilon_1)$ are,

$$\begin{aligned} &\lambda_1 = -0.859517, \lambda_2 = -0.778, \lambda_3 = 0.322, \lambda_4 = -0.2863, \\ &\lambda_5 = -0.078, \lambda_6 = -0.078, \lambda_7 = 0.0244172, \lambda_8 = -0.0071. \end{aligned}$$

We conclude that ϵ_1 is unstable since $\lambda_7 > 0$. The linearized matrix of the System (15) on ϵ_2 is constructed using the same technique,

$$J(\epsilon_2) = \begin{bmatrix} -0.118 & 0.063 & 0.063 & -0.548 & 0.063 & 0.062 & 0 & -0.263 \\ 0.019 & -0.873 & -0.028 & -0.038 & -0.028 & -0.028 & 0 & 0.263 \\ 0.004 & -0.007 & -0.293 & 0.115 & -0.007 & -0.007 & 0 & 0 \\ 0.018 & -0.026 & -0.026 & -0.026 & -0.027 & -0.026 & 0 & -0.006 \\ -0.001 & 0.015 & -0.001 & 0.02 & -0.78 & -0.001 & 0 & 0.006 \\ 0 & 0.15 & 0.1853 & 0.2 & 0.5 & -0.078 & 0 & 0 \\ 0.0008 & -0.022 & 0.0007 & 0.0007 & 0.0008 & 0.0008 & -0.027 & 0 \\ -0.0008 & 0.022 & -0.0007 & -0.0008 & -0.0008 & -0.0008 & 0.0204 & -0.0071 \end{bmatrix}. \tag{17}$$

with eigenvalues,

$$\begin{aligned} &\lambda_1 = -0.875 + i,\ \lambda_2 = -0.78 + I,\ \lambda_3 = -0.286 + i,\ \lambda_4 = -0.078 + 0.123i, \\ &\lambda_5 = -0.0785 - 0.123i,\ \lambda_6 = -0.08 + i,\ \lambda_7 = -0.018 + i,\ \lambda_8 = -0.0071 + i. \end{aligned}$$

We can determine that ϵ_2 is locally asymptotically stable given a set of parameters such that $\mathcal{R}_0$ since all of the real components of the eigenvalues are negative.

4 Numerical simulation

We explored the analytical behaviors of the entire model in previous sections (1). Following that, we will conduct a model simulation. We also use the initial values of the state variables for the model equations provided in Table 2, and the parameter values are addressed in the relevant figures.

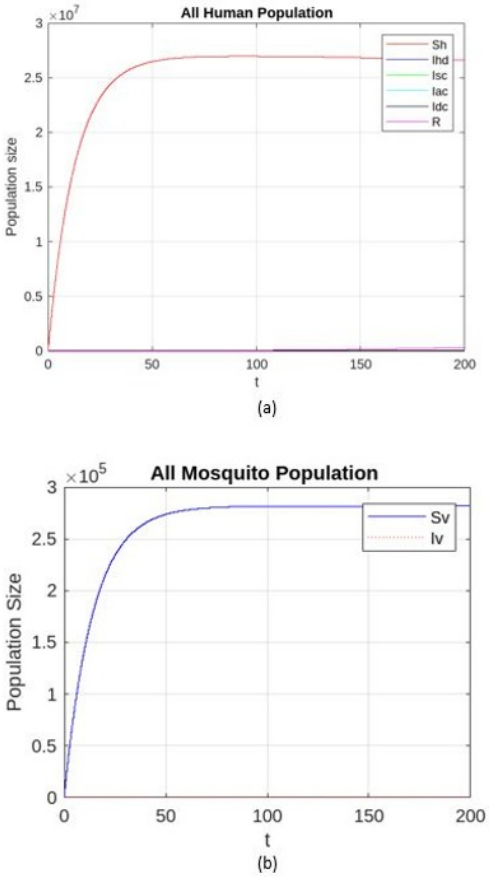

Fig. 2. Dynamic solutions of the coinfection Model (1), with parameter values $\beta_{VD} = 0.42, \beta_{HD} = 0.6$, $\beta_{AC} = 0.8$ $\alpha_1 = 0.15$,$\alpha_3 = 0.2$, and $\gamma_{AC} = 0.2$, then its basic reproduction number is $\mathcal{R}_0 = 0.643 < 1$.

The previous section presented the subsystem's analytical findings (2). We now provide the numerical solutions for state variables based on the initial conditions $S_H(0) = 5000$, $I_H D(0) = 1000$, $I_A C(0) = 1000$, $I_S C(0) = 1000$, $I_D C(0) = 1000$, $R(0) = 10$, $S_V(0) = 1000$, $I_V(0) = 10$, consider the parameters specified in each figure.

Then it can be seen, Fig. 2 shows a coinfection COVID-19-Dengue solution with the parameter values shown in the caption. The basic reproduction number of coinfection model is $\mathcal{R}_{0C} = 0.643$, indicating that the disease-free equilibrium point is stable and that there is no endemic equilibrium point. Figure 2 illustrates that the susceptible population approaches the value of $\frac{\theta_H}{\mu_H}$, whilst the other compartments approach zero, confirming our analytical results from earlier sections. As time passes, the solutions in Fig. 3 come closer to the endemic equilibrium point, which has a basic reproduction number greater than one, which agrees with the analytical properties.

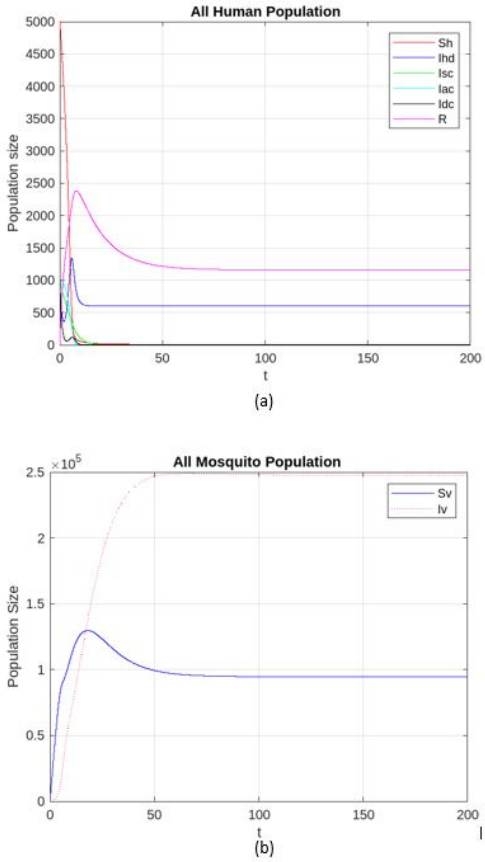

Fig. 3. Dynamic solutions of the coinfection Model (1), with parameter values $\beta_{VD} = 0.2, \beta_{HD} = 0.2$, $\beta_{AC} = 0.5$ $\alpha_1 = 0.15$, $\alpha_3 = 0.3$, and $\gamma_{AC} = 0.2$, then its basic reproduction number is $\mathcal{R}_0 = 2.138 > 1$.

5 Conclusion

In this study, we develop a new mathematical model for Dengue-COVID-19 coinfection by taking into consideration both asymptomatic and symptomatic COVID-19 infections. The human population is split into six compartments, while the mosquito population is split into two. The model was built as an 8-dimensional system of nonlinear ordinary differential equations.

The model was qualitatively examined by separating it into two subsystems: the dengue infection system and the COVID-19 infection system. Furthermore, we calculated their equilibrium points and examined their stability in relation to the basic reproduction numbers. We demonstrated that when the respective basic reproduction numbers are less than one, the disease-free equilibrium points in both subsystems are stable. When the basic reproduction numbers are bigger than unity, the disease-free equilibrium point becomes unstable, and our numerical simulation shows that there exists a single endemic equilibrium point that is locally asymptotically stable.

When the basic reproduction number is less than one, the entire Dengue-COVID-19 coinfection model provides a disease-free equilibrium point that is locally asymptotically

stable. To support the analytical results, various simulation cases were run, and the results were found to be in good agreement.

Several investigations have been conducted to better understand the coinfection of COVID-19 and dengue fever, [21] and [5] concentrate on preventing COVID-19 coinfection by preventing dengue and COVID-19, they do not take into account the population infected with COVID-19, who can be both symptomatic and asymptomatic case. Different from previous research, this research investigates the possibility of that case occurring. However, the present study has some limitations. To avoid model complexity, symptomatic classes of COVID-19 do not cause coinfection. In reality, not all humans infected with symptomatic COVID-19 are isolated so there is a possibility of coinfection. They can be included in further research.

Acknowledgements

The authors acknowledge Directorate of Research and Development, Universitas Indonesia for all support of this research (Hibah PUTI Q2 - Batch 3 with addendum No. NKB-1458/UN2. RST/HKP.05.00/2022).

References

1. H. Li, S.M. Liu, X.H. Yu, S.L. Tang, C.K. Tang, Int. J. Antimicrob. Agents **55**, 105951 (2020)
2. WHO, *Modes of transmission of virus causing covid-19: implications for ipc precaution recommendations: scientific brief*, 29 March 2020, Available at : https://www.who.int/news-room/commentaries/detail/modes-of-transmission-of-virus-causing-covid-19-implications-for-ipc-precaution-recommendations
3. S. Wongkoon, M. Jaroensutasinee, K. Jaroensutasinee, Indian J. Med. Res. **138**, 347 (2013)
4. M. Verduyn et al., PLOS Negl. Trop. Dis. **14**, e0008476 (2020)
5. M.A. Hye, M.H.A. Biswas, M.F. Uddin, M. Saifuddin, Comput. Math. Model. **33**, 173 (2022)
6. A. Saipen, B. Demot, L. De Leon, Western Pac. Surveill. Response J. **12**, 35 (2021)
7. M.G. Guzman, D.J. Gubler, A. Izquierdo, E. Martinez, S.B. Halstead, Nat. Rev. Dis. Primers **2**, 1 (2016)
8. D. Aldila, M.Z. Ndii, N. Anggriani, H. Tasman, B.D. Handari, Alex. Eng. J. **64**, 691 (2023)
9. R.H. Al-Rifai et al., PLoS One **16**, e0246903 (2021)
10. S. Lee et al., JAMA Intern. Med. **180**, 1447 (2020)
11. G. Yin, H. Jin et al., JMIR Public Health Surveill. **6**, e19464 (2020)
12. J.P. Arcede, R.L. Caga-Anan, C.Q. Mentuda, Y. Mammeri, Math. Model. Nat. Phenom. **15**, 34 (2020)
13. I. Ahmed, G.U. Modu, A. Yusuf, P. Kumam, I. Yusuf, Results Phys. **21**, 103776 (2021)
14. M. Biswas et al., Comput. Model. Eng. Sci. **125**, 1033 (2020)
15. K.G. Mekonen, S.F. Balcha, L.L. Obsu, A. Hassen, J. Appl. Math. **2022**, 1 (2022)
16. I.M. Hezam, A. Foul, A. Alrasheedi, Adv. Differ. Equ. **2021**, 1 (2021)
17. H.T. Alemneh, Adv. Differ. Equ. **2020**, 664 (2020)
18. F. Özköse, M. Yavuz, Comput. Biol. Med. **141**, 105044 (2022)
19. N. Ringa et al., Inform. Med. Unlocked. **31**, 100978 (2022)

20. E. Bonyah, M.A. Khan, K.O. Okosun, J. Gómez-Aguilar, Optim. Control Appl. Methods **40**, 394 (2019)
21. A. Omame, H. Rwezaura, M. Diagne, S. Inyama, J. Tchuenche, Eur. Phys. J. Plus **136**, 1090 (2021)
22. O. Diekmann, J. Heesterbeek, M.G. Roberts, J. R. Soc. Interface. **7**, 873 (2010)
23. T. Hens et al., *On the stability of intertemporal equilibria with rational expectations* (Citeseer, Bonn, 1994)
24. Z.S. Kifle, L.L. Obsu, Heliyon **9**, e18726 (2023)
25. S.M. Garba, A.B. Gumel, M.A. Bakar, Math. Biosci. **215**, 11 (2008)
26. A. Omame, M.E. Isah, M. Abbas, Optim. Control Appl. Methods **44**, 170 (2023)
27. K.O. Okuneye, J.X. Velasco-Hernandez, A.B. Gumel, J. Biol. Syst. **25**, 545 (2017)
28. K.G. Mekonen, T.G. Habtemicheal, S.F. Balcha, Results Appl. Math. **9**, 100134 (2021)